Nature Environment and Pollution Technology
An International Quarterly Scientific Journal

ISSN: 0972-6268	Vol. 15	No. 3	pp. 805-816	2016

Original Research Paper

Distributions of Water Droplet Penetration time and Soil Properties Under Point Source Trickle Irrigation Using Treated Wastewater

Yi Li*† and Yanling Shang**
*College of Water Resources and Architecture Engineering, Northwest A&F University, Yangling , Shaanxi, 712100, China
**Guanyinge Reservoir Management Bureau, Liaoning, 117100, China
†Correspondence: Yi Li

Nat. Env. & Poll. Tech.
Website: www.neptjournal.com

Received: 03-09-2015
Accepted: 16-12-2015

Key Words:
Point source trickle irrigation
Soil water repellency
Soil water distribution
Soil salt distribution
Contour map

ABSTRACT

Treated wastewater irrigation (TWWI) is necessary under the background of a worldwide water crisis. To investigate wetting patterns and distributions of water droplet penetration time (WDPT), soil water content (θ), soil organic matter (SOM) and salt content (S) after tap water irrigation (TWI) and TWWI, single-point-source trickle irrigation experiments were conducted on sandy and loam soils at three flow rates of 0.6, 1.0 and 2.7 mL·min^{-1}. For sand, infiltration was generally regular, WDPT increased small with maximal value of 1.4 s, and the ratio of wetting fronts (R_w) decreased to 1.1 with time. For loam soil, infiltration was not as regular as sand, R_w decreased with time, but larger than 1.5, WDPT increased significantly after TWWI, with maximal increment of 34.2 s at 1.0 mL·min^{-1}, and the distributions of SOM and S were irregular especially at flow rates of 2.7 mL·min^{-1}. SOM was not the main cause of the increment of WDPT for both soil types. Values of θ and S were considered to have contributed to the increment of WDPT for saline-alkali loam soil after TWI and TWWI. Particle content, especially sand content also affected WDPT. WDPT interacted with soil properties during TWW and TWWI.

INTRODUCTION

Trickle-irrigation represents one of the fastest expanding technologies in modern irrigated agriculture with a great potential for achieving efficient water use (Lubana & Narda 2001). Discharge rate, spacing between emitters, diameter and length of the lateral system are important design parameters for trickle irrigation systems, along with the percentage of root zone to be wetted, frequency and amount of irrigation as well as depth of installation (Cook et al. 2006). The wetted soil volume, wetted radius or vertical and lateral wetting front advances (Acar et al. 2009), and soil water and solute distributions were concerned when studying wetting patterns of trickle irrigation. There are different models for estimation of wetting patterns from point sources, presented by Schwartzman & Zur (1986), Chu (1994), Roth (1974), Zur (1996), Li et al. (2004), and Bar-Yosef & Sheikholslami (1976). Besides the mathematical models, numerical solution was also useful (Bhatnagar 2008) and the software such as WetUp (Cook et al. 2006) and HYDRUS (Simunek et al. 2006) were popularly applied.

The use of treated municipal wastewater in irrigation is one of the effective measures for coping with water shortage in regions poor in water resources. It is considered an environmentally sound wastewater disposal practice compared to its direct disposal to the surface or groundwater bodies (Mohammad 2003). Bernier et al. (2013) reported that short-term treated wastewater (TWW) irrigation (for 5 years) of the clay from Yifa, resulted in intense soil organic matter degradation and depletion of both the aliphatic CH and hydrophilic groups. TWW irrigation (TWWI) has an impact on the chemical and hydraulic properties of soils (Lado & Ben-Hur 2009). TWW was also found to induce soil water repellency (SWR) under prolonged irrigation with treated sewage effluent (Wallach et al. 2005). TWW contains higher contents of electrolytes, dissolved organic matter, suspended solids, and biochemical and chemical oxygen demand (DeBano 1981), which may contribute to the development and increase of hydrophobicity (Mataix-Solera et al. 2011) which was hard to be eliminated even after 6 years. During the infiltration into effluent irrigated soils which were severely repellent, infiltration rates were very low at the beginning compared with infiltration rates in the wettable and slightly repellent soils and then increased; this confirmed the effects of effluent-irrigation on the development of SWR (Wallach & Graber 2007). Travis et al. (2008) found a significant increase of SWR in sandy and loam soils after irrigated with raw artificial grey water within 40 days. Arye et al. (2011) found that SWR only exhibited in the surface soil layer after TWWI.

The development of SWR or hydrophobicity is a dynamic process in both the short and long term conditions. Therefore, it exhibits temporal-spatial variability, particularly under recurrent and frequent irrigation events. The re-establishment of hydrophobicity, following irrigation or a rain event, is strongly time-dependent and likely to diminish or even disappear (Arye et al. 2011). Because SWR may lead to increased surface runoff (Burch 1989), soil erosion (Shakesby 2000) and fingered preferential flow (Ritsema 1997), its development, distributions and possible causes should be correctly assessed. Although there were research focusing on the wetting patterns and hydrophobicity characteristics during TWWI, the mechanics of soil wettability and hydrophobicity under TWWI was still not clear, more researches are needed due to the complicated feature of soil hydrophobicity.

This research aims to: (1) compare the effects of various *q* values of TW and TWW trickle irrigation on the wetting patterns and the distributions of SWR, contents of soil water, SOM and salt within the wetted zones at a given emitter spacing of 30 cm; (2) discuss how soil hydrophobicity differs for different soils; and (3) analyse the related soil properties that affects SWR. The obtained results may help people understand SWR more and to ameliorate low-quality soils during TWWI practice.

MATERIALS AND METHODS

Levels of SWR and basic properties of the tested soils and irrigation water: One of the most common methods of classifying SWR is to determine the time a water drop takes to be absorbed by the soil sample. The measured values of WDPT longer than 5 seconds are desirable for obtaining information on the persistency of hydrophobicity (DeBano 1981). Mataix-Solera et al. (2011) presented a detailed classification of hydrophobicity from levels of 0 to 9.

Two types of soils, including a sand and a loam soil were collected from the top 30 cm of the fields from two sites in China. Sands were taken from the first terrace of Weihe River bank in Yangling, Shaanxi, China. Loam soils were taken from a field in Manasi County in Xinjiang Autonomous Region, China. All the soils were placed in the cloth bags and transported to the laboratory. The soil samples were air-dried, ground, and passed through a 2 mm sieve. Initial WDPT ($WDPT_i$) values for the air-dried sieved samples were measured using a stopwatch, averaged by WDPT values of eight water droplets. Soil particle contents were measured by the pipette method. Soil textures were classified according to the USDA classification system. Soil electrical conductivity (EC) for the saturation extract solution was measured via a DDS-303A conductivity meter with water and soil ratio of 5:1 (Bao 2000). Soil organic matter (SOM) was measured using oil bath heating-potassium dichromate volumetric method. Measurements of initial WDPT ($WDPT_i$), SOM and EC were similar with those for the soil samples taken after infiltration experiments in section 2.3. The initial physical-chemical characteristics of the tested soils are listed in Table 2. Loam soil was considered moderately saline, while sand was non-saline.

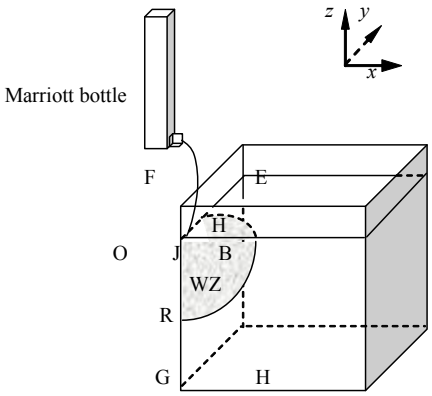

Fig. 1: Experimental system of point source trickle irrigation using tap water and treated waste water. The emitter is 5mm above the O position. WZ-wetted zone.

Table 1: Initial physico-chemical characteristics of the applied treated wastewater. TWW- Treated wastewater, CSV- China Standard Value.

Item	COD ($mg \cdot L^{-1}$)	BOD ($mg \cdot L^{-1}$)	SS ($mg \cdot L^{-1}$)	pH	TN	TP
TWW	118.1	71.6	21.1	7.54	25.7	3.98
Tap water	2.8	0.9	1.7	7.2	-	-
CSV	200	100	100	-	-	-

TWW for the trickle irrigation was collected from Huayu Water Quality Purification Limited Corporation located in the south of Yangling, Shaanxi, China. TWW was filtered to pass a 2-mm-in-diameter screen mesh before it was utilized in the experiments. pH value for the TWW was measured using an EL20K pH-meter, chemical oxygen demand (COD) was measured using fast digestion-spectrophotometric method, biochemical oxygen demand (BOD) was measured using standard dilution method, and the initial suspended substance was measured using gravimetric method (Dai 2010). The sewage water has been secondary treated and qualified for farmland irrigation standards in China (GB5084-2005). The measured chemical characteristics of the tap water (TW) and TWW are given in Table 1.

Laboratory point-source drip infiltration experiments: Trickle infiltration experiments were conducted using a steady rest, a 5 cm-in-diameter Marriott bottle and a 30 cm ×

Table 2: Particle contents and initial soil property. The particle size of clay, silt and sand ranges from <0.001mm, 0.001~0.05mm and 0.05~0.2mm, respectively. $WDPT_i$ - initial WDPT, EC - electrical conductivity, SOM - soil organic matter, BD - bulk density.

Soil	Clay (%)	Silt (%)	Sand (%)	Soil texture	$WDPT_i$ (s)	EC ($\mu s \cdot cm^{-1}$)	SOM ($g \cdot kg^{-1}$)	BD ($g \cdot cm^{-3}$)	Na^+ ($g \cdot kg^{-1}$)	Mg^{2+} ($g \cdot kg^{-1}$)	Ca^{2+} ($g \cdot kg^{-1}$)
Sandy	0.1	6.2	93.7	Sand	1.5	38.7	5.69	1.60	0.25	0.11	0.09
Saline-alkali	22.8	31.9	45.3	Loam	2.0	623.7	7.38	1.45	3.18	0.32	1.07

Table 3: The maximal and average increments of WDPT in *xoz* block for the tested soils. TWI-tap water irrigation, TWWI- treated wastewater irrigation (similar below).

Soil	Irrigation	Average increment of WDPT at q (s)			Maximal increment of WDPT at q (s)		
		0.6	1.0	2.7	0.6	1.0	2.7
Sandy	TWI	0.3	0.2	0.5	0.6	0.5	0.7
Sandy	TWWI	0.6	0.7	0.9	0.8	1.0	1.4
Loam	TWI	6.7	6.2	5.2	15.1	11.3	8.2
Loam	TWWI	10.8	12.9	12.7	24.2	34.2	18.3

30 cm × 30 cm volume soil box made up of transparent Plexiglas (Fig. 1). There were small circular holes in the bottom wall of the soil box. A filter paper was put on the bottom of it. The Marriott bottle was connected to a needle, which was fixed at the inner corner of soil box, downward rightly 0.5 cm above the soil surface. The pre-calibrated application rates were 0.6, 1.0 and 2.7 $mL \cdot min^{-1}$, respectively.

The initial soil water contents were 0.023 $cm^3 \cdot cm^{-3}$ for sand and 0.036 $cm^3 \cdot cm^{-3}$ for loam soil. Soils were packed to the Plexiglas box layer by layer to soil height of 25 cm. The bulk densities were 1.6 $g \cdot cm^{-3}$ for sands and 1.4 $g \cdot cm^{-3}$ for loam soils referring to the former experiments conducted on these soils. A stopwatch was started for recording infiltration time when the water dropped to soil surface. Cumulative infiltration was observed from the decreased water volume within the observation time span. The wetting front was observed visually through the box wall.

The experiments were stopped after 1440 min of infiltration for sand, after 1440 min at *q* values of 0.6 and 1.0 $mL \cdot min^{-1}$ for loam soil, but stopped after 180 min at *q* of 2.7 $mL \cdot min^{-1}$ for loam soil because of the heavy ponding of water on soil surface and uneven distribution of water. Soil samples of wetted zone were taken radially at a 5 cm interval in the *xoy* planes as quickly as possible. Soil moisture was measured using oven dry method. Soil samples were ground and prepared for extract solution using 1:5 ratio of soil to water, which was also done in the initial soil property measurement (Table 2). Soil saturation extract EC was measured using a DDS-303A type EC meter. The relationship between *EC* ($\mu s \cdot cm^{-1}$) and soil salt content (*S*, g kg^{-1}) is:

$$S=0.03EC-11.03,\ R^2=0.994 \quad ...(1)$$

SOM was measured using oil bath heating - potassium dichromate volumetric method. WDPT values were measured for all the soil samples immediately after they were oven-dried at 75°C, averaged by WDPT values of eight droplets for each sample. Surfer 8.0 software was applied to draw contour maps of soil properties. Pearson correlation coefficient (*r*) was used to assess the statistical connections between WDPT and soil properties.

Wetting parameters: The ratio of wetting front in the direction *x* ($z_{f,x}$) to that in the direction *z* ($z_{f,z}$), denoted by R_w, indicates the relative infiltration speed in different directions. R_w is described as a power function of infiltration time based on the observed data:

$$R_w = z_{f,x} / z_{f,z} = at^b \quad ...(2)$$

Where *a* and *b* are fitted parameters. R_w varied during infiltration.

The volume of the wetted zone (*V*) of sand is calculated as a 1/8 spheroid:

$$V = \frac{4\pi}{3}\left(\frac{z_{f,x,\max} + z_{f,y,\max} + z_{f,z,\max}}{3}\right)^3 / 8 = \frac{\pi}{6} z_{f,ave}^3 \quad ...(3)$$

Where $z_{f,x,\max}$, $z_{f,y,\max}$ and $z_{f,z,\max}$ are the maximal wetting fronts in the *x*, *y* and *z* directions of the wetted zone; $z_{f,ave}$ is the average radius of the final wetted zone.

Truncated ellipsoid shape (Zur 1996) is assumed for loam soil. *V* is calculated by:

$$V = \frac{4\pi}{3}(z_{f,x,\max} \cdot z_{f,y,\max} \cdot z_{f,z,\max}) / 8 = \frac{\pi}{6}(z_{f,x,\max} \cdot z_{f,y,\max} \cdot z_{f,z,\max}) \quad ...(4)$$

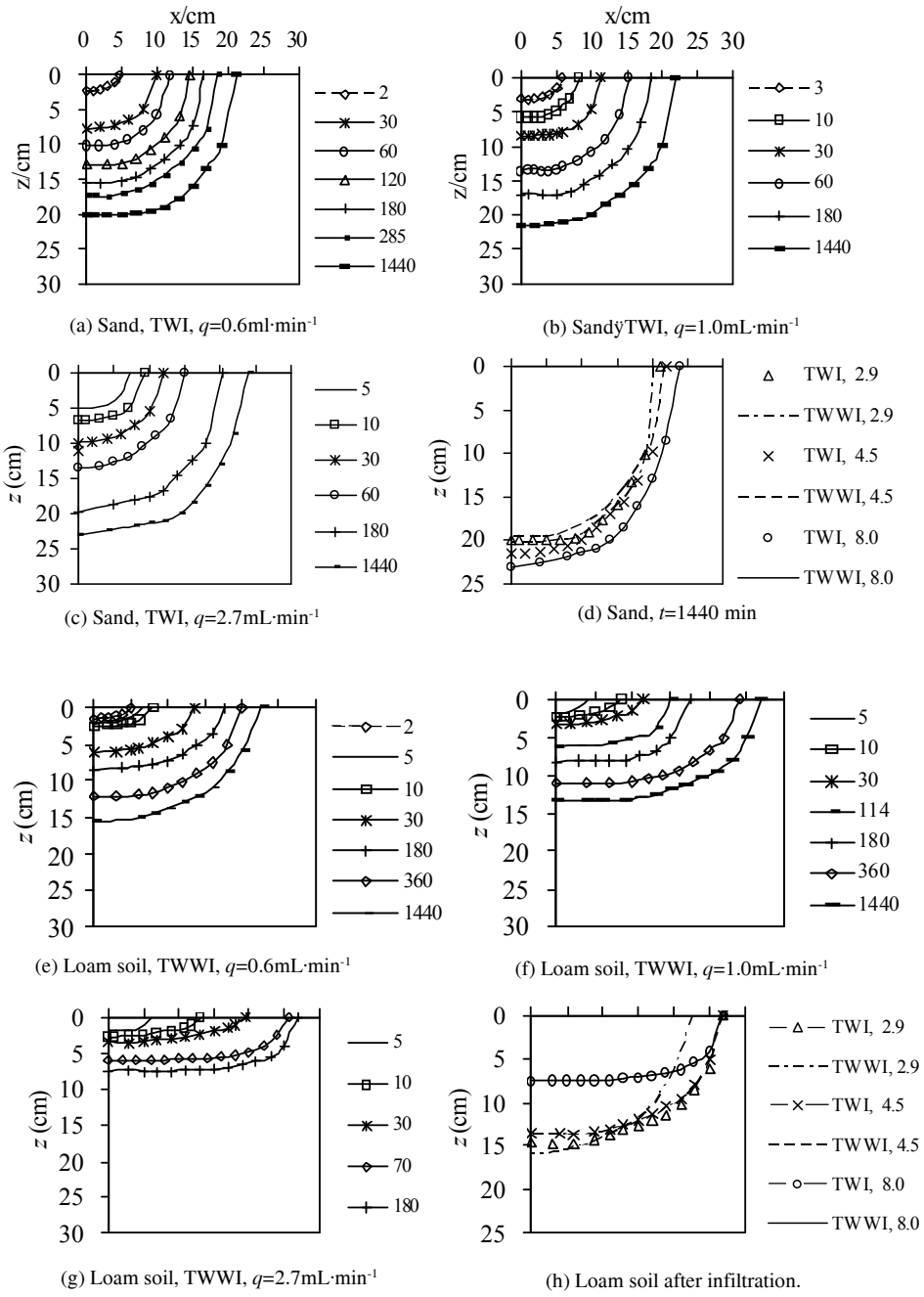

(a) Sand, TWI, q=0.6ml·min^{-1} (b) SandÿTWI, q=1.0mL·min^{-1}

(c) Sand, TWI, q=2.7mL·min^{-1} (d) Sand, t=1440 min

(e) Loam soil, TWWI, q=0.6mL·min^{-1} (f) Loam soil, TWWI, q=1.0mL·min^{-1}

(g) Loam soil, TWWI, q=2.7mL·min^{-1} (h) Loam soil after infiltration.

Fig. 2: Wetting front advances for TWI and TWWI for the tested soils. TWI-tap water irrigation, TWWI-treated wastewater irrigation (similar below). The legends in a, b, c, e, f, and g denote the infiltration time (t, min) and in d&h denote discharge rate (q, mL·min^{-1}).

The average soil water content (θ_{ave}) is determined by

$$\theta_{ave} = (W - V_p) / V \quad ...(5)$$

Where, W is the water applied to the soil volume, mL; V_p is the volume of ponded water on the soil surface, mL. V_p for sand is 0, V_p for loam soil is determined by W multiplying coefficient C_{vp} varying between 0 and 0.3. C_{vp} for q of 0.6, 1.0 and 2.7 mL·min^{-1} for loam soil were 0.09, 0.15 and 0.2 for tap water irrigation (TWI), and were 0.2, 0.3 and 0.3 for TWWI according to the estimated area of ponded region during experiments. C_{vp} for sand was 0.

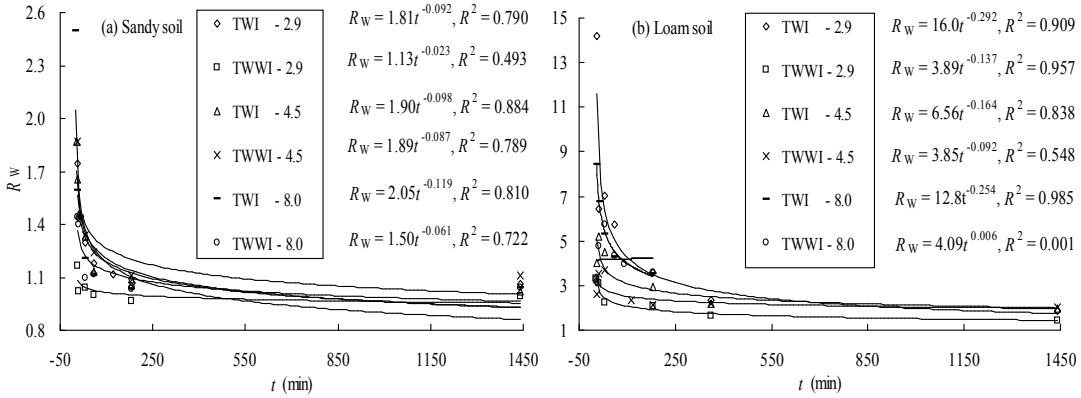

Fig. 3: R_w of the tested soils for TWI and TWWI at various q values.

RESULTS

Effects of TWW point source trickle irrigation on wetting patterns: Wetting fronts are observed visually (Fig. 2). For sand, $z_{f,x}$ and $z_{f,z}$ advanced almost similarly when the time elapsed and the wetting front generally took 1/4 of sphere shapes at all of the three q values. The final $z_{f,x}$ ($z_{f,z}$) were 21.2, 22 and 26 cm (20, 21.5 and 25.7cm) for 0.6, 1.0 and 2.7 mL·min^{-1} of TWI at 1440 min, respectively. There were small differences between z_f of TWI and TWWI at the same q values. Generally, the larger the discharge rates, the longer z_f. Wetting fronts for sand were regular at various q values. z_f of q from 0.6, 1.0 to 2.7 mL·min^{-1} increased slower, because soil matrix potentials at the wetting edges were smaller and smaller as water moved farther from emitter. Values of θ_{ave} were larger when q increased.

For loam soil, $z_{f,x}$ was larger than $z_{f,z}$ from the beginning to the end of the infiltration, and the differences between them were the largest at 180 min for q of 2.7 mL·min^{-1} compared to the other q. The final $z_{f,x}$ and $z_{f,z}$ were similar for TWI and TWWI when q were 1.0 and 2.7 mL·min^{-1}, but differed a lot when q was 0.6 mL·min^{-1}. The reason that $z_{f,x}$ differed with $z_{f,z}$ obviously at 0.6 mL·min^{-1} was that the infiltration for loam soil was irregular, even q was small as 0.6 mL·min^{-1}, there was ponding water on soil surface. There was heavier ponded water as q increased. At q of 2.7 mL·min^{-1}, water ponding was so heavy that water was hard to infiltrate deeper but more flowed laterally on soil surface. Preferential flow was observed, so there were only data before 180 min in Fig. 2g. z_f in the x and y directions were visually different and irregular. At 1440 min for q of 0.6 mL·min^{-1}, the irregularity of wetting front advances may be amplified compared to those at 180 min for q of 2.7 mL·min^{-1}, although there was similarity of wetting front advances for q of 1.0 mL·min^{-1}.

The z_f for sand agreed with the results of Acar et al. (2009) and Mostaghami et al. (1981), who concluded that larger the emitter discharges, the more the vertical wetting front advance. Overall, the wetting front advances for loam soil were more complicated than those for sand.

R_w values and the fitted parameters a and b (Eq. 2) under TWI and TWWI are shown in Fig. 3. Fig. 3 showed that: (1) R_w decreased as infiltration time prolonged. (2) For sand, the largest R_w was 2.5, appearing at the t of 1min for q of 2.7 mL·min^{-1} under TWI. R_w decreased to 1.1 at the end of the infiltration. R_w values varied between 0.99 and 1.1 at 1440 min. The coefficients of determination (R^2) for fitting equation 2 ranged between 0.78 and 0.88 of TWI treatments and were larger than R^2 values for TWWI treatments which ranged between 0.49 and 0.79. (3) For loam soil, the largest R_w was 14.2, appearing at t of 5 min for q of 0.6 mL·min^{-1} under TWI. R_w decreased were around 3.1 for q of 2.7 mL·min^{-1} at 180 min. R_w values varied between 1.45 and 2.0 for q of 0.6 and 1.0 mL·min^{-1} at 1440 min, indicating that the wetting plane of xoz were not like that of sand any more (circles), but shaped more like a ellipse. R^2 for describing R_w

Table 4: The volume of the wetted zone and the average soil water content θ_{ave} after TWI and TWWI for the tested soils.

Soil	Irrigation	q (mL min^{-1})	V(cm^3)	W (mL)	V_p (mL)	θ_{ave} (cm^{3}cm^{-3})
Sandy	TWI	0.6	4667	864	0	0.19
Sandy	TWI	1.0	5400	1440	0	0.27
Sandy	TWI	2.7	9062	3888	0	0.43
Sandy	TWWI	0.6	4252	864	0	0.20
Sandy	TWWI	1.0	4735	1440	0	0.30
Sandy	TWWI	2.7	9381	3888	0	0.41
Loam	TWI	0.6	5594	864	43	0.15
Loam	TWI	1.0	5780	1440	288	0.20
Loam	TWI	2.7	3092	486	97	0.13
Loam	TWWI	0.6	4190	864	86	0.19
Loam	TWWI	1.0	5077	1440	432	0.20
Loam	TWWI	2.7	2831	486	97	0.14

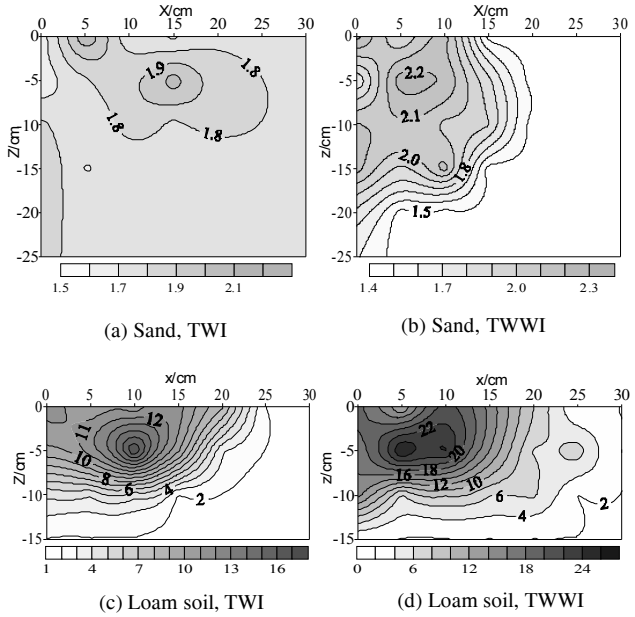

(a) Sand, TWI (b) Sand, TWWI

(c) Loam soil, TWI (d) Loam soil, TWWI

Fig. 4: Contour maps of *WDPT* in the *xoz* block at q of 0.6 mL·min^{-1} and t of 1440 min.

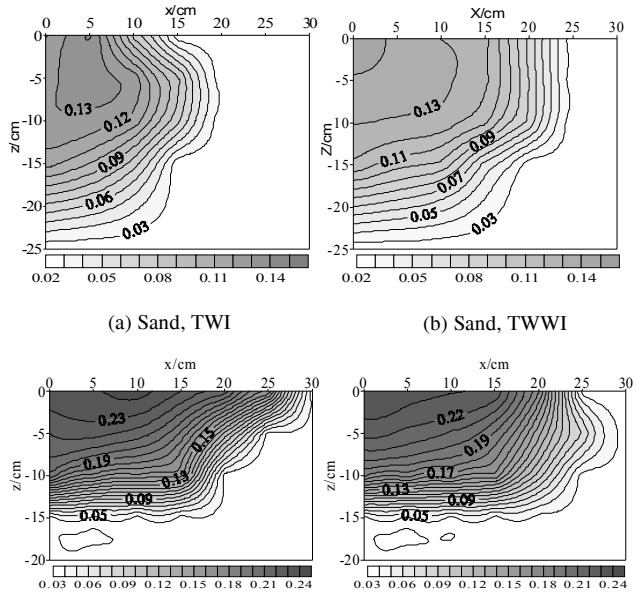

(a) Sand, TWI (b) Sand, TWWI

(c) Loam soil, TWI (d) Loam soil, TWWI

Fig. 5: Contour maps of soil water content (cm^3 cm^{-3}) in the *xoz* block at q of 0.6 mL·min^{-1} and t of 1440 min.

in terms of t ranged between 0.83 and 0.98 for TWI treatments and were larger than R^2 values for TWWI treatments which ranged between 0.001 and 0.96. R^2 value for q of 2.7 mL·min^{-1} under TWWI was very low (0.001) because R_w fluctuated between 3.15 and 5.76 and scattered around 4 within the short infiltration time of 180 min. (4) R_w values for sand were smaller than those for loam soil.

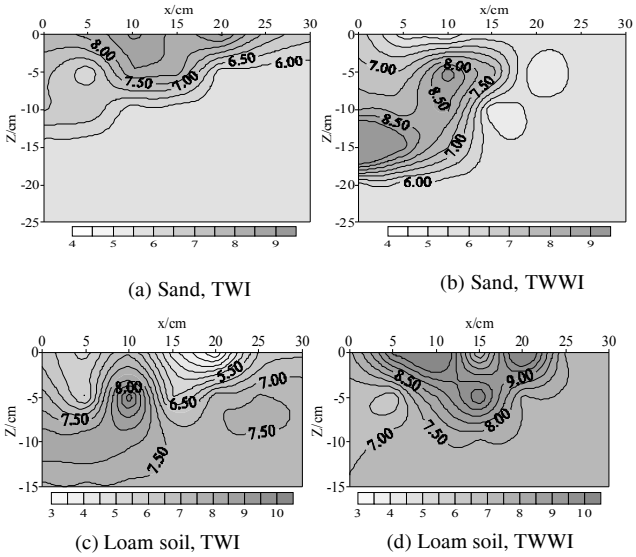

(a) Sand, TWI (b) Sand, TWWI

(c) Loam soil, TWI (d) Loam soil, TWWI

Fig. 6: Contour maps of SOM (g kg^{-1}) in the *xoz* block at q of 0.6 mL·min^{-1} and t of 1440 min.

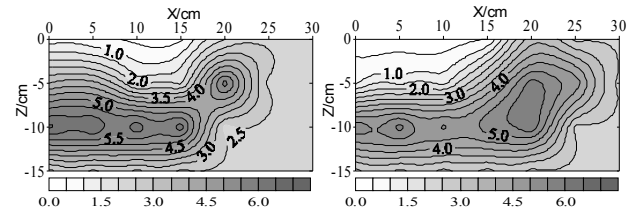

(a) Loam soil, TWI (b) Loam soil, TWWI

Fig. 7: Contour maps of S (g kg^{-1}) in the *xoz* block at q of 0.6 mL·min^{-1} and t of 1440 min.

Distributions of WDPT on the *xoz* plane: WDPT contour maps in the *xoz* block at q of 0.6 mL·min^{-1} for sand and loam soils are illustrated as a demonstration in Fig. 4. Counter maps of WDPT for sand at other q values were not shown and could refer to q of 0.6 mL·min^{-1}, because the infiltration behaviour of sand was generally regular. WDPT was 1.5 s for sand initially but increased after TWI and TWWI (Figs. 4a and 4b). WDPT increased small (less than 1.4 s) in the wetted zone after TWI and TWWI. The increment of WDPTs for TWWI were larger than for TWI and the increment of WDPTs for q of 2.7 mL·min^{-1} were larger than for q of 0.6 and 1.0 mL·min^{-1}. In spite of the increase of WDPTs, the hydrophobicity level of sand after TWI and TWWI was still maintained at level 0. Whatever, after TWI or TWWI, the whole wetted zone for sand was wettable.

WDPT values increased obviously for loam soils (Figs. 4c and 4d). WDPT values were large at the middle zone of the radius from the emitter, shaping like a circular belt. The maximal WDPT values were located around depth of 5 cm

Table 5: Pearson correlation coefficients (r) for WDPT and soil properties. TTSP- Two tailed significance probability. * denotes passing the two tailed significance test at the significance level of 0.05. ** denotes passing the two tailed significance test at the significance level of 0.001.

Soil	Irrigation	WDPT~ SOM		WDPT~ θ		WDPT ~ S	
		r	TTSP	r	TTSP	r	TTSP
Sand	TWI	0.034	0.655	0.361	0.129	-0.203	0.405
Sand	TWWI	-0.015	0.861	0.557**	0	-0.370*	0.011
Loam	TWI	-0.099	0.303	0.751**	0	-0.626**	0
Loam	TWWI	-0.260*	0.047	0.576**	0	-0.572**	0

but farther than 5 cm from the origin in the x direction. WDPT values at wetting fronts were small and close to $WDPT_i$. The distributions of WDPT in the *xoz* block were almost in ellipse shapes for q values of 0.6 and 1.0 mL·min^{-1}, but were almost rectangular at q of 2.7 mL·min^{-1}. At the same discharge rates, WDPT increments were larger for TWWI than for TWI. As q values increased from 0.6 to 1.0 mL·min^{-1}, WDPT increased more for TWWI than for TWI. WDPT increment was found smaller at t of 180 min than at 1440 min, which implied that long-time TWWI manifested stronger repellency persistence than short-time irrigation.

WDPT increment for sand was small but for loam soil was relatively large, although t was not longer than 1440 min. For further understanding of WDPT increment characteristics, the average and maximal WDPT increment values for the tested soils are given in Table 3.

The WDPT increment between TWI and TWWI for sand differed little, either average or maximal values, ranging between 0.2 and 1.4 s. It was clear that the short time infiltration of TWW had no notable effects on WDPT and hydrophobicity level of sand. WDPT increment for loam soil was remarkable after a short time TWI and TWWI. The average increments of WDPT were between 5.2 and 6.7 s for TWI and between 10.8 and 12.9 s for TWWI, but differed small at various q values. The maximal increments of WDPT were between 8.2 and 15.1 s for TWI and between 18.3 and 34.2 s for TWWI. Both average and maximal increments of WDPT for loam soils were larger than those for sand. After infiltration, the initially wettable loam soil become hydrophobic and the hydrophobicity level increased from 0 to 1, 2 and 3 at various positions of the wetted zone. TWWI influenced changes of WDPT more at any q values than TWI for loam soil.

Distributions of soil water content in the *xoz* block: Contour maps of θ in the *xoz* block at q of 0.6 mL·min^{-1} for sand and loam soil (Fig. 5) are shown as a demonstration. The distributions of θ for sand were generally regular and in spherical shapes at different q values, which were similar to the WDPT distributions (Figs. 5a and 5b). The larger the q values, the larger the θ at the positions below the emitter. The distributions of θ for loam soil were in elliptical shapes at q values of 0.6 (Figs. 5c and 5d) and 1.0 mL·min^{-1}, but almost in rectangular shapes at q of 2.7 mL·min^{-1}. There was slight ponding of water at the surface of loam soil at a small q but heavy ponding at a large q. The distributions of θ followed those of wetting fronts and there were interactions between soil water and SWR.

For further comparisons, the calculated wetted volume (V) and average soil moisture (θ_{ave}) for the tested soils are presented in Table 4. For sand, V ranged from 4252 to 9381 cm^3 and θ_{ave} ranged from 0.19 to 0.43 cm^3 cm^{-3}. For loam soil, V ranged from 2831 to 5780 cm^3 and θ_{ave} ranged from 0.15 to 0.20 cm^3 cm^{-3}. θ_{ave} for loam soil was much smaller than for sand. Moreover, θ_{ave} for TWI was a little smaller than for TWWI.

Distributions of soil organic matter and soil salt content in the *xoz* block: SOM changes after the trickle infiltration. The contour maps of SOM (Fig. 6) in the *xoz* block are obtained. SOM distributed following the water flow directions but distributed irregular in the wetted zone both for sandy and loam soils, which were different with distributions of WDPT and θ. The average SOM for TWI were almost equal to initial SOM. The average SOM in *xoz* block for TWWI were 7.64, 7.95 and 8.41 g kg^{-1} for sand and 8.39, 9.31 and 7.88 g kg^{-1} for loam soil when q increased from 0.6 to 1.0 and to 2.7 mL·min^{-1}, respectively. Average SOM values for TWWI were larger than those for TWI because of SOM input from TWW. SOM increment for loam soil at q of 2.7 mL·min^{-1} was small because of its small infiltration caused by surface water ponding.

Sand's soil salt content (S) is very low, so the distributions of S won't be discussed. The distributions of S for loam soil in the *xoz* block are shown in Fig. 7. The distributions of S were affected by the surface ponded water. S values were smaller than 1.0 g kg^{-1} at upper 5 cm depth. Radial distributions of S were obvious at q of 0.6 and 1.0 mL·min^{-1}. There were peak values of S inside the wetting front. The leaching areas with low S were larger at q of 1.0 mL·min^{-1} than at 0.6 mL·min^{-1}, also larger for TWWI than TWI. At q of 2.7 mL·min^{-1}, the distribution of S was irregular with almost rec-

tangular shapes because of surface heavy ponded water both for TWI and TWWI.

The connections between WDPT and the related soil properties: Variations of WDPT vs SOM, S and θ after infiltration are shown in Fig. 8. Increase in SOM did not definitely result to an obvious increase of WDPT (Figs. 8a to 8d) both for TWI and TWWI and for sand and loam soil. Noting that sand was taken from Weihe river bank with initial low SOM of 5.69 g kg^{-1}, although TWWI increased the average WDPT value compared to TWI, it was still wettable. TWI and TWWI changed the distributions of SOM and also increased the WDPT in the blocks of loam soil, but there were no direct connections between WDPT and SOM, which were different with some of the former researches. WDPT generally decreased when S increased for loam soil both after TWI and TWWI (Figs. 8e to 8f). WDPT values for TWWI were generally larger than 5 s compared to $WDPT_i$ of 2.0 s. WDPT increased obviously for loam soil after infiltration, this was not reported previously. The increase in θ could be a reason of the increase in WDPT. Increase in WDPT was more obvious for loam soil rather than for sand (Figs. 8g to 8j). De Jonge et al. (1999) generalized curve type with no SWR at any θ(I), single-peak curve type (II) and double-peak curve type (III). Our results agree with De Jonge et al. in that WDPT~θ curve for sand belonged to curve type I and that for loam soil belonged to a part of curve type II. Therefore WDPT~ θ curves for sandy and loam soils were considered normal.

Pearson correlation coefficients (r) for assessing the statistically linear correlation relationship between WDPT and soil properties are given in Table 5. For sand during TWI, the correlations for WDPT with SOM, θ and S were all statistically insignificant, indicating the weak connections between WDPT and soil properties. Correlation between WDPT and SOM was statistically insignificant for sand and at TWI condition for loam soil. But at TWWI condition for sand as well as at TWI and TWWI conditions for loam soil, the correlations between WDPT and θ as well as S were statistically significant and passed two-tail test, indicating the close connections between them. Generally, absolute values of r were larger for loam soil than for sand, which implied that SOM, θ and S contributed more to the development of SWR for loam soil than for sand after infiltration.

The connections between WDPT and soil properties including SOM, θ and S were complicated. For wettable sand, WDPT increased very slightly with various SOM and θ and its hydrophobicity level was not changed either by TWI or TWWI. For loam soil which was saline-alkali, WDPT increased largely and its wettability changed from wettable to water repellent. The increase in θ and the decrease in S, caused by water movement during infiltration, contributed more than SOM to the increment of WDPT for loam soil.

DISCUSSION

Factors related to soil water repellency: SWR is a dynamic process (Doerr & Thomas 2000). Its re-establishment to a certain degree after thorough wetting through irrigation or rainfall is strongly time dependent (Tarchitzky et al. 2007). Its breakdown can be due to unusual characteristics of soil-low bulk density (0.8 Mg m^{-3}), strongly aggregated nature, presence of mycorrhizal fungi, high SOM content (16.5%), or presence of allophonic clay (4%) Clothier (2000). Among the factors influencing SWR, organic matter (OM) induces WR by several means (DeBano 1981). Changes in the OM characteristics of a thin soil layer (0-2 cm) at the surface of the soil profile were considered to relate to hydrophobicity in TWW-irrigated soil (Tarchitzky et al. 2007). Soil moisture is also an important factor that influences SWR (Doerr & Thomas 2000). In this research, both TWI and TWWI increased WDPT of loam soils for either short (180 min) or long time (1440 min), but changes in WDPT for sand were small. For sand, SOM played minor roles in changing SWR, the reason was that sand samples were taken from Weihe river bank, where much of SOM were flushed away by water percolated from the Weihe river. Moreover, most SOM is insoluble and requires a strong alkaline solution to be removed from soils. The low SOM in TWW also didn't play much role in increasing water repellency persistence for sand. It's reasonable that our results for sand were different from the former research (Dekker & Ritsema 1994, Dekker et al. 2001).

Considering the small contributions of initial low SOM to SWR of sand and loam soils, SOM was not the major factor influencing SWR in this research, but soil salt and the other components of TWW (which may increase the chemical substances in soils and indirectly increase S after infiltration) were believed to be also responsible for the increment of WDPT for loam soils beside soil moisture, which could be testified by the generally high Pearson correlation coefficients between WDPT and θ and S for loam soils after infiltration. But the contributions of other related factors, such as COD, pH values and BOD in TWW and soils are still not clear.

Infiltration of hydrophobic soils was smaller than wettable soils (Feng et al. 2001, 2002). The heavy ponded surface water of loam soils changed the distributions of WDPT, SOM, θ and S. The low infiltration ability and irregular distributions of θ were accompanied with the ponding water, which was seen apparently from the wetted volumes

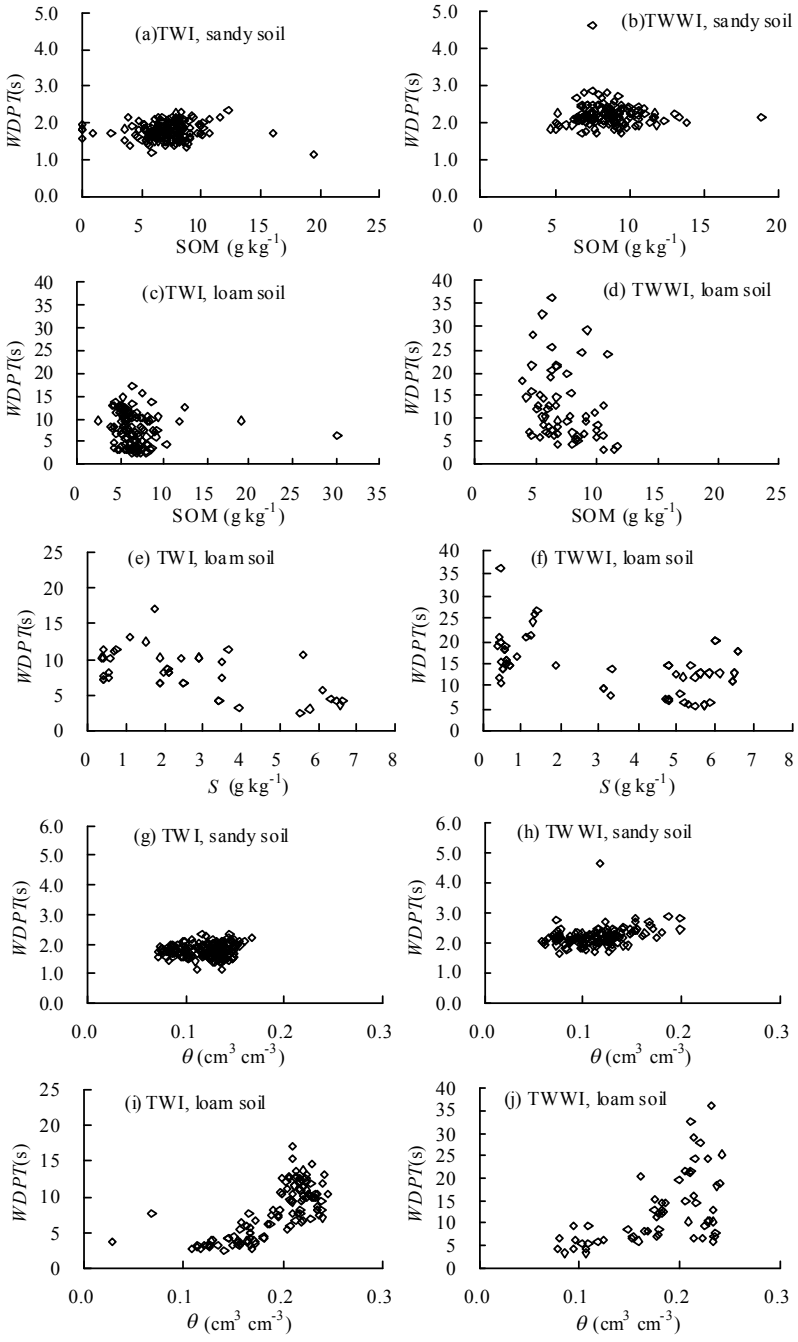

Fig. 8: Relationship between *WDPT* and SOM, soil salt content (S) and water content (θ).

of loam soils compared to sand at the similar discharge rates. Similar ponding water phenomenon caused SWR (Tarchitzky 2007). Since the infiltration characteristics affect the root adsorption water of crops, SWR plays negative roles in increasing water use efficiency during irrigation practice and are strongly recommended to be one of the design parameters in the trickle irrigation systems.

Because the distributions of θ for sand were generally regular and there was no ponding water at the soil surface at various q values in this research, 2.7 mL·min^{-1} or larger q could be selected as the rational discharge rate for sand. In contrast to sand, q of 0.6 mL·min^{-1} or smaller values was

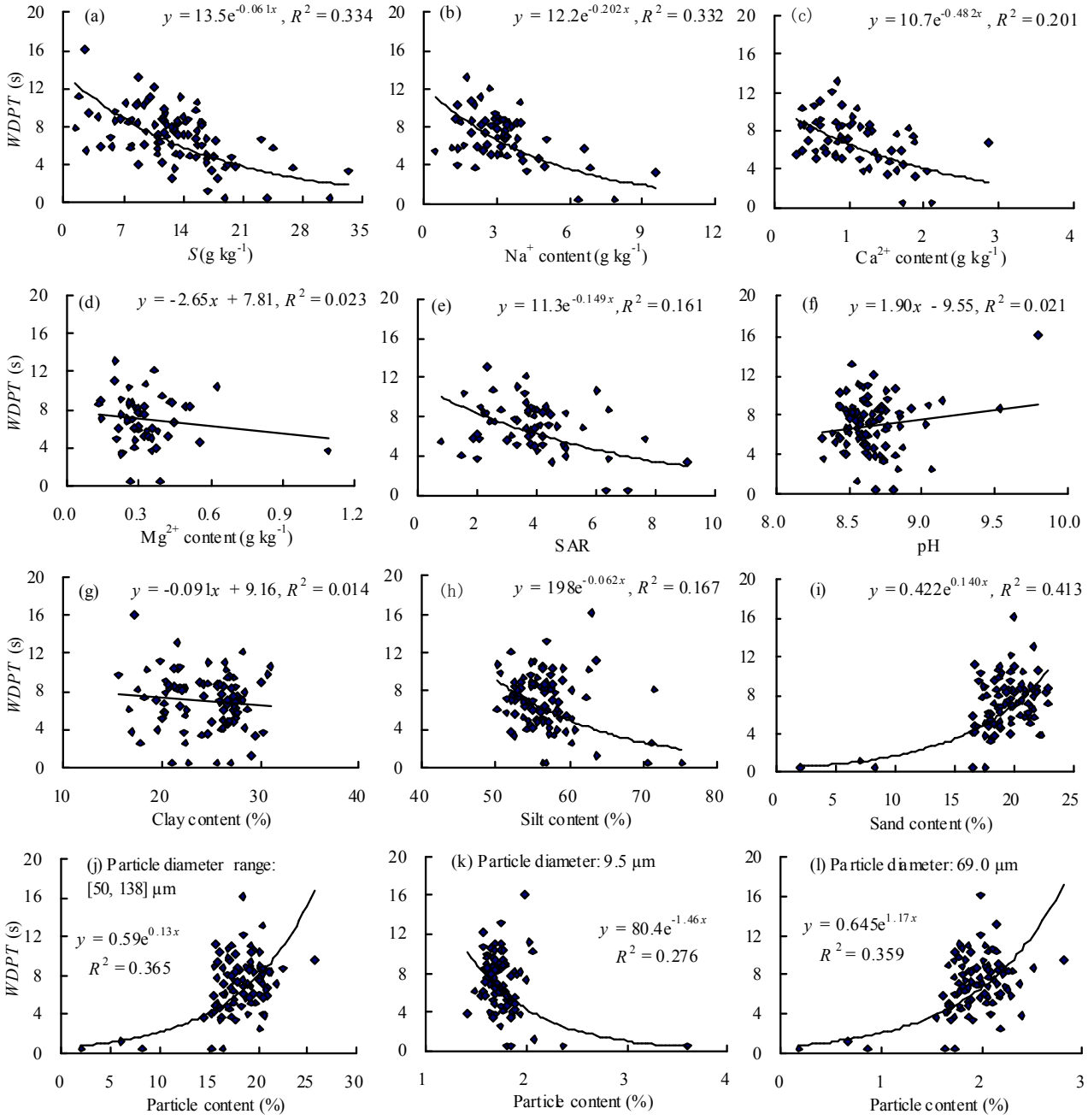

Fig. 9: WDPT variations with chemical properties and particle contents for loam soil.

recommended for loam soil in trickle irrigation.

Contribution of salinity and particle size distributions on water repellency of loam soil: Contributions of salinity properties to WDPT were larger than SOM for loam soil in this research, which was unexpected because SOM was reported to have played important roles in affecting SWR (Doerr & Thomas 2000). Noting that the initial SOM values of the studied sandy and loam soils were only 5.69 and 7.38 g kg^{-1}, such low SOM affected variations of WDPT little. So it was not a surprise that SOM didn't show obvious effects on WDPT of both soils. It is also necessary to mention that the initial *S* of sandy and loam soil in the infiltration experiments differed a lot, being 0.23 and 7.68 g kg^{-1}, respectively. So that for loam soil, *S* could be one of the factors that caused

the variations of WDPT.

The obtained field data related to SWR for loam soil could be an extra proof to show the effects of S on WDPT. Loam soil was taken from a field which was fallow in 1980s because of heavy salinization caused by mismanagement of irrigation. The field was re-cultivated, planted with cotton and irrigated by trickle emitters from 2007. Total 90 soil samples were taken along transect with a 10-cm interval at soil depth of 0 to 20 cm in July, 2007 (Li 2010). Particle size distributions were measured using a Longbench Mastersizer 2000 (Malvern Instruments, Malvern, England) (Li et al. 2011). S was measured using gravimetric method. The contents of Na^+, Ca^{2+} and Mg^{2+} were measured using a Hitachi 180-80 atomic absorption spectrometer (Bao 2000). Sodium adsorption ratio (SAR) was calculated by:

$$SAR = \frac{Na^+}{\sqrt{0.5(Ca^{2+} + Mg^{2+})}}$$

The variations of WDPT with the observed saline properties and particle contents are shown in Fig. 9. The soil samples were spatially distributed in the field, which was different with the homogeneous soils used for the laboratory infiltration experiments.

WDPT decreased when all of the studied saline parameters decreased (Figs. 9a to 9e). S explained 33.4% of the variations of WDPT (R^2=0.334), of which Na^+, Ca^{2+} and Mg^{2+} played an important, a next important and a minor role in WDPT values with R^2 values of 0.332, 0.201 and 0.023, respectively. WDPT also decreased with the increase in SAR, but the correlation between them was not good (R^2=0.161). WDPT increased with the increase in pH values, but there was an even lower correlation between the two properties (R^2=0.021) (Fig. 9f).

WDPT decreased slightly with the increase in clay and silt contents, but increased with the increase in sand content (particle diameter range [50, 2000] μm) (Figs. 9g to 9i). Changes of particle content, especially sand content affected WDPT values of loam soil. When sand content increased from 17 to 25%, there was an obvious increase in WDPT from 5 to 18 s. Particle content of different diameter also played different roles in affecting WDPT. WDPT increased with the increase in sand content at a narrower diameter range [50, 138] μm (Fig. 9h). WDPT values were also sensitive to the changes of particle contents at diameter ranges [1.6, 10.6] μm. Specifically, WDPT decreased with the increase in particle contents at a diameter of 9.5 μm and increased with the increase in particle contents at a diameter of 69.0 μm (Figs. 9k and 9L). In general, particle content at diameter range [50, 138] μm explained most of WDPT increase for loam soil.

As mentioned above, there were different factors affecting increase of WDPT of loam soil, such as θ, S and particle content. Section 3 explained intrinsic mechanics of WDPT variations caused by the movements of soil water, organic matter and salt after TWI and TWWI. Section 4.2 displayed how WDPT changes with particle contents, soil salt and ion contents in a relative static space. It was concluded that WDPT interacted with soil properties under different soil and irrigation conditions. WDPT changes during infiltration were caused by the movement of water, which changed the variations of SOM, θ, S and ion contents, etc. Water quality was one of the factors affecting WDPT. Soil texture and initial soil properties such as soil EC or salt content, SOM, etc., were also important factors affecting WDPT.

CONCLUSIONS

The wetting fronts and the distributions of soil water under TW and TWW point source trickle infiltration were regular for sand. The larger the discharge rates, the longer and deeper the wetting fronts, and the higher the wetted soil volume and average soil moisture. WDPT for sand increased a little but the levels of hydrophobicity were still in 0 after TWI and TWWI. The increment of WDPT for sand was small. SOM contributed small to the slight increase in WDPT for sand.

The wetting fronts of loam soil were not as regular as sand after TWI and TWWI, so were the distributions of SOM, θ and S. WDPT increased remarkably after TWI and TWWI. TWWI influenced WDPT more at any q values than TWI for loam soil. Increase in θ and decrease in S were important factors that caused the increment of WDPT. The increase of sand content caused an increase of WDPT for loam soil. Particle content, especially sand content at diameter range [50, 138] μm was also the important factors that affect WDPT. SWR is an important property and interacted with soil water, salt and SOM movement under different soil and irrigation conditions. SWR is strongly recommended to be considered in the design of irrigation systems.

ACKNOWLEDGEMENTS

The financial support of Projects includes the China National Natural Science Foundation (51579213) and the China 111 Project (Grant No. B12007).

ABBREVIATIONS

Pearson correlation coefficient-r; q-application rate; t-infiltration time; TW-tap water; TWW-treated wastewater; TWI-Tap water irrigation; TWWI-treated wastewater irrigation; WDPT-water droplet penetration time; SWR-soil water repellency; $WDPT_i$-initial WDPT; SOM-soil organic

matter ; EC-electrical conductivity; θ-soil water content; θ_{ave} -average soil moisture; *S*-soil salt content; R_w-ratio of wetting front in the direction *x* ($z_{f,x}$) to that in the direction *z* ($z_{f,z}$); *V*-volume of the wetted zone; WZ-wetted zone; SAR-sodium adsorption ratio.

REFERENCES

Acar, B., Topak, R. and Mikailsoy, F. 2009. Effect of applied water and discharge rate on wetted soil volume in loam or clay-loam soil from an irrigated trickle source. Afr. J. Agric. Res., 4(1): 49-54.

Arye, G., Tarchitzky, J. and Chen, Y. 2011. Treated wastewater effects on water repellency and soil hydraulic properties of soil aquifer treatment infiltration basins. J. Hydrol., 397: 136 -145.

Bao, S. D. 2000. Soil and agricultural chemistry analysis. China Agricultural Press, Beijing (in Chinese).

Bar-Yosef, B. and Sheikholslami, M.R. 1976. Distribution of water and ions in soils irrigated and fertilized from a trickle source. Soil Sci. Soc. Am. J., 40(4): 575-582.

Bernier, M., Levy, G. J., Fine, P. and Borisover, M. 2013. Organic matter composition in soils irrigated with treated wastewater: FT-IR spectroscopic analysis of bulk soil samples. Geoderma, 209-210: 233-240.

Bhatnagar, P.R. and Chauhan, H. S. 2008. Soil water movement under a single surface trickle source. Agric. Water Manag., 95: 799-808.

Burch, G. J., Moore, I. D. and Burns, J. 1989. Soil hydrophobic effects on infiltration and catchment runoff. Hydrol. Process., 3: 211-222.

Chu, S. T. 1994. Green-ampt analysis of wetting patterns for surface emitter. J. Irrig. Drainage Eng. ASCE., 120: 414-421.

Clothier, B. E., Vogeler, I. and Magesan, G. N. 2000. The breakdown of water repellency and solute transport through a hydrophobic soil. J. Hydrol., 231-232: 255-264.

Cook, F. J., Fitch, P., Thorburn, P. J., Charlesworth, P. B. and Bristow, K. L. 2006. Modelling trickle irrigation: comparison of analytical and numerical models for estimation of wetting front position with time. Environ. Modell. Softw., 21: 1353-1359.

Dai, J.Q. 2010. Water analytical chemistry experiment. China Petrochemical Press, Beijing (in Chinese).

De Jonge, L. W., Jacobsen, O. H. and Moldrup, P. 1999. Soil water repellency: effects of water content, temperature and particle size. Soil Sci. Soc. Am. J., 63: 437-442.

DeBano, L. F. 1981. Water repellent soils: a state-of-art. Pacific Southwest For. Range Exp. Stn. Gen. Tech. Rep., PWW-46: 21pp.

Dekker, L. W. and Ritsema 1994. How water moves in a water repellent sand: I. Potential and actual water repellency. Water Resour. Res., 30 (9): 2507-2517.

Dekker, L. W., Doerr, S. H., Oostindie, K., Ziogas, A. K. and Ritsema, C. J. 2001. Water repellency and critical soil water content in a dune sand. Soil Sci. Soc. Am. J., 65: 1667-1674.

Doerr, S. H. and Thomas, A. D. 2000. The role of soil moisture in controlling water repellency: new evidence from forest soils in Portugal. J. Hydrol., 231-232: 134-147.

Feng, G. L., Letey, J. and Wu, L. 2001. Water ponding depths affect temporal infiltration rates in a water-repellent sand. Soil Sci. Soc. Am. J., 65: 315-320.

Feng, G. L., Letey, J. and Wu, L. 2002. The influence of two surfactants on infiltration into a water-repellent soil. Soil Sci. Soc. Am. J., 66: 361-367.

Lado, M. and Ben-Hur, M. 2009. Treated domestic sewage irrigation effects on soil hydraulic properties in arid and semiarid zones: A review. Soil Till. Res., 106: 152-163.

Li, J., Zhang, J. and Rao, M. 2004. Wetting patterns and nitrogen distributions as affected by fertigation strategies from a surface point source. Agric. Water Manag., 67: 89-104.

Li, M. 2010. Spatial variability of fractal dimensions for soil particle size distributions and physical properties. MSC Thesis, Northwest Agriculture and Forestry University, Yangling, China (in Chinese with English Abstract).

Li, Y., Li, M., Horton, R. 2011. Single and joint multifractal analysis of soil particle size distributions. Pedosphere, 21(1): 75-83.

Lubana, P. P. S. and Narda, N.K. 2001. Modelling soil water dynamics under trickle emitters-a review. J. Agric. Engng. Res., 78(3): 217-232.

Mataix-Solera, J., García-Irles, L., Morugán, A., Doerr, S.H., Garcia-Orenes, F., Arcenegui, V., Atanassova, I. 2011. Longevity of soil water repellency in a former wastewater disposal tree stand and potential amelioration. Geoderma, 165(1): 78-83.

Mohammad, M.J. and Mazahreh, N. 2003. Changes in soil fertility parameters in response to irrigation of forage crops with secondary treated wastewater. Comm. Soil Sci. Plant Anal., 34(9 & 10): 1281-1294.

Mostaghami, S., Mitchell, K. J. and Lembke, W.D. 1981. Effect of discharge rate on distribution of moisture in heavy soils irrigated from a trickle source. Trans. ASAE., 25: 2081-2085.

Ritsema, C. J., Dekker, L. W. and Heijs, A. W. J. 1997. Three-dimensional fingered flow patterns in a water repellent sandy field soil. Soil Sci., 162(2): 79-90.

Roth, R. L. 1974. Soil moisture distribution and wetting pattern from a point-source. Proceeding of the Second International Drip Irrigation Congress, pp. 246-256.

Schwartzman, M. and Zur, B. 1986. Emitter spacing and geometry of wetted soil volume. J. Irrig. Drainage Eng. ASCE., 112: 242-253.

Shakesby, R. A., Doerr, S.H. and Walsh, R. P. D. 2000. The erosional impact of soil hydrophobicity: current problems and future research directions. J. Hydrol., 231-232: 178-191.

Simunek, J., van Genuchten, M. T. and Sejna, M. 2006. The HYDRUS software package for simulating two- and three-dimensional movement of water, heat, and multiple solutes in variably saturated media. Technical Manual, Version 1.0, PC Progress, Prague, Czech Republic, pp. 241.

Tarchitzky, J., Lerner, O., Shani, U., Arye, G., Lowengart-Aycicegi, A., Brener, A. and Chen, Y. 2007. Water distribution pattern in treated wastewater irrigated soils: hydrophobicity effect. Eur. J. Soil Sci., 58: 573-588.

Travis, M.J., Weisbrod, N. and Gross, A. 2008. Accumulation of oil and grease in soils irrigated with grey water and their potential role in soil water repellency. Sci. Total Environ., 394: 68-74.

Wallach, R., and Graber, E.R. 2007. Infiltration into effluent irrigation-induced repellent soils and the dependence of repellency on ambient relative humidity. Hydrol. Process., 21: 2346-2355.

Wallach, R., Ben-Arie, O. and Graber, E.R. 2005. Soil water repellency induced by long-term irrigation with treated sewage effluent. J. Environ. Qual., 34: 1910-1920.

Zur, B. 1996. Wetted soil volume as a design objective in trickle irrigation. Irrig. Sci., 16: 101-105.